Brain Research Bulletin, Vol. 29, pp. 783–793, 1992
Printed in the USA.

0361-9230/92 $5.00 + .00

Distribution of Calbindin D-28K and Parvalbumin Immunoreactivities in the Nucleus Olfactorius Anterior of the Rat

E. GARCÍA-OJEDA, J. R. ALONSO,[1] R. ARÉVALO, J. G. BRIÑÓN, J. LARA AND J. AIJÓN

Departamento de Biología Celular y Patología, Facultad de Biología, Universidad de Salamanca, 37007-Salamanca, Spain

Received 31 March 1992; Accepted 26 April 1992

GARCÍA-OJEDA, E., J. R. ALONSO, R. ARÉVALO, J. G. BRIÑÓN, J. LARA AND J. AIJÓN. *Distribution of calbindin D-28K and parvalbumin immunoreactivities in the nucleus olfactorius anterior of the rat.* BRAIN RES BULL **29**(6) 783–793, 1992.—The distributions of calbindin D-28K (CaBP) and parvalbumin (PV) in the rat nucleus olfactorius anterior (NOA) were described using monoclonal antibodies and the avidin-biotin-peroxidase method. The NOA showed a high immunoreactivity for CaBP, with a rostrocaudal increase in the positive neurons and fibres. Pars externa (NOAe) was the only subdivision which showed a low CaBP immunostaining. PV-positive elements were less abundant that those CaBP immunostained. The main difference in the distributions for both proteins was observed in the pars medialis which was practically PV negative. PV- and CaBP-stained neurons showed similar morphologies in the subdivisions where they were present. In NOAe, we observed a characteristic PV- and CaBP-positive neuronal type, with an oriented dendritic pattern. Transition areas were clearly observable in both CaBP- and PV-labelled sections.

Calbindin D-28K Parvalbumin Calcium binding Immunocytochemistry Rat

CALCIUM ions are an important intracellular second messenger involved in neurotransmission and membrane excitability. Calcium-binding proteins are a group of small molecules which posses specific cavities to accept this ion with large affinity and selectivity (5,25). In most calcium-binding proteins the physiological function is still unknown, although it has been postulated that they constitute a potent intracellular buffering mechanism to restrict and restore the calcium physiological levels (7,19).

Calbindin D-28K and parvalbumin are two buffer calcium-binding proteins which are useful in Neurohistology, because they are present, among other locations, in specific neuronal populations, widely distributed in the central nervous system. The presence of these calcium-binding proteins has been proved in the rat brain using different techniques, including immunocytochemistry, radioimmunoassay, and in situ hybridization (3,8,11,13,18,26,32).

The nucleus olfactorius anterior (NOA) establishes connections with a variety of olfactory-related brain structures such as: contra- and ipsilateral olfactory bulb, contralateral NOA, piriform cortex, taenia tecta, entorhinal cortex, amygdaloid nuclei, horizontal and vertical diagonal band, endopiriform nuclei, bed nucleus of the stria terminalis, and tuberomammillary hypothalamus (23). It represents the second structural unit of the olfactory system, enabling the cross coordination of the olfactory information received in both olfactory epithelia, allowing that the same sensory information arrive to both hemispheres (10,20,21,28,30,34).

The aims of this work were to study the distribution patterns of CaBP and PV in the rat NOA, describing the immunoreactivity in the different NOA subdivisions and the morphology of the stained elements, comparing them with previous reports on the distribution of these proteins in the rat and human NOA.

METHOD

Ten adult female Wistar rats weighing between 180–280 g were used in this study. The animals were anesthetized with intraperitoneal injections of 6% sodium pentobarbital (0.01 ml/kg body weight). The rats were transcardially perfused first with Ringer solution followed by a fixative mixture of 15% saturated picric acid, 4% paraformaldehyde, and 0.08% glutaraldehyde in 0.1 *M* phosphate buffer pH 7.2 (PB) (33). The brains were removed and placed in the same fixative without glutaraldehyde for 5 h and transferred to 30% sucrose in PB (vol/vol) at 4°C overnight.

The pieces containing the nucleus olfactorius anterior were cut at a thickness of 30 μm perpendicularly to the longitudinal axis of the brain with a cryostat. The free-floating sections were

[1] Requests for reprints should be addressed to Dr. J. R. Alonso, Departamento de Biología Celular y Patología, Avda. Campo Charro s/n., 37007 Salamanca, Spain.

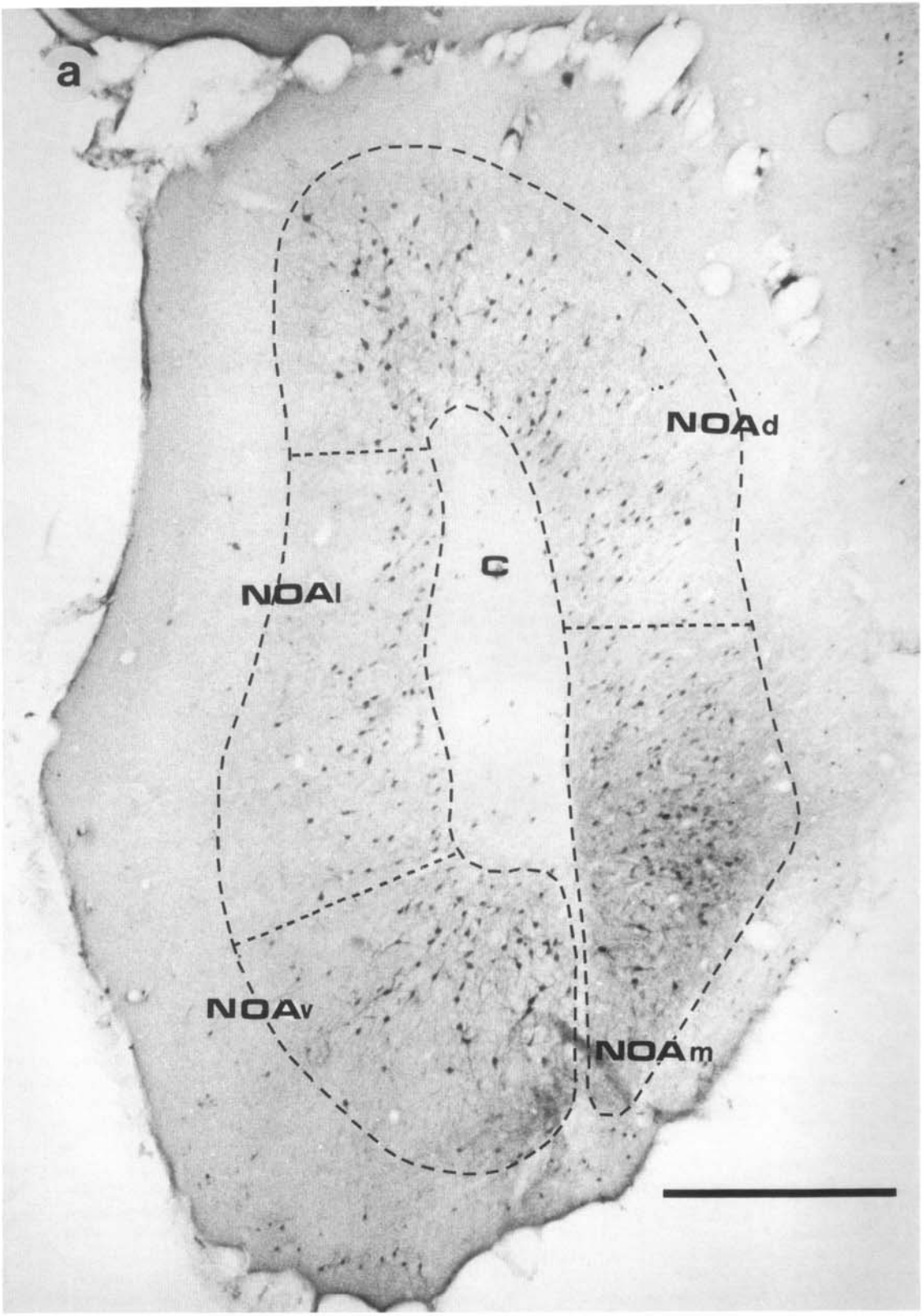

ABOVE AND FOLLOWING PAGE:

FIG. 1. CaBP and PV immunoreactivity. Bregma level 4.70. Panoramic frontal sections showing CaBP (a) and PV (b) immunoreactivities. Note the higher density of CaBP elements than PV ones and the absence of PV structures in NOAm. (C = commissure). Scale bar = 500 μm.

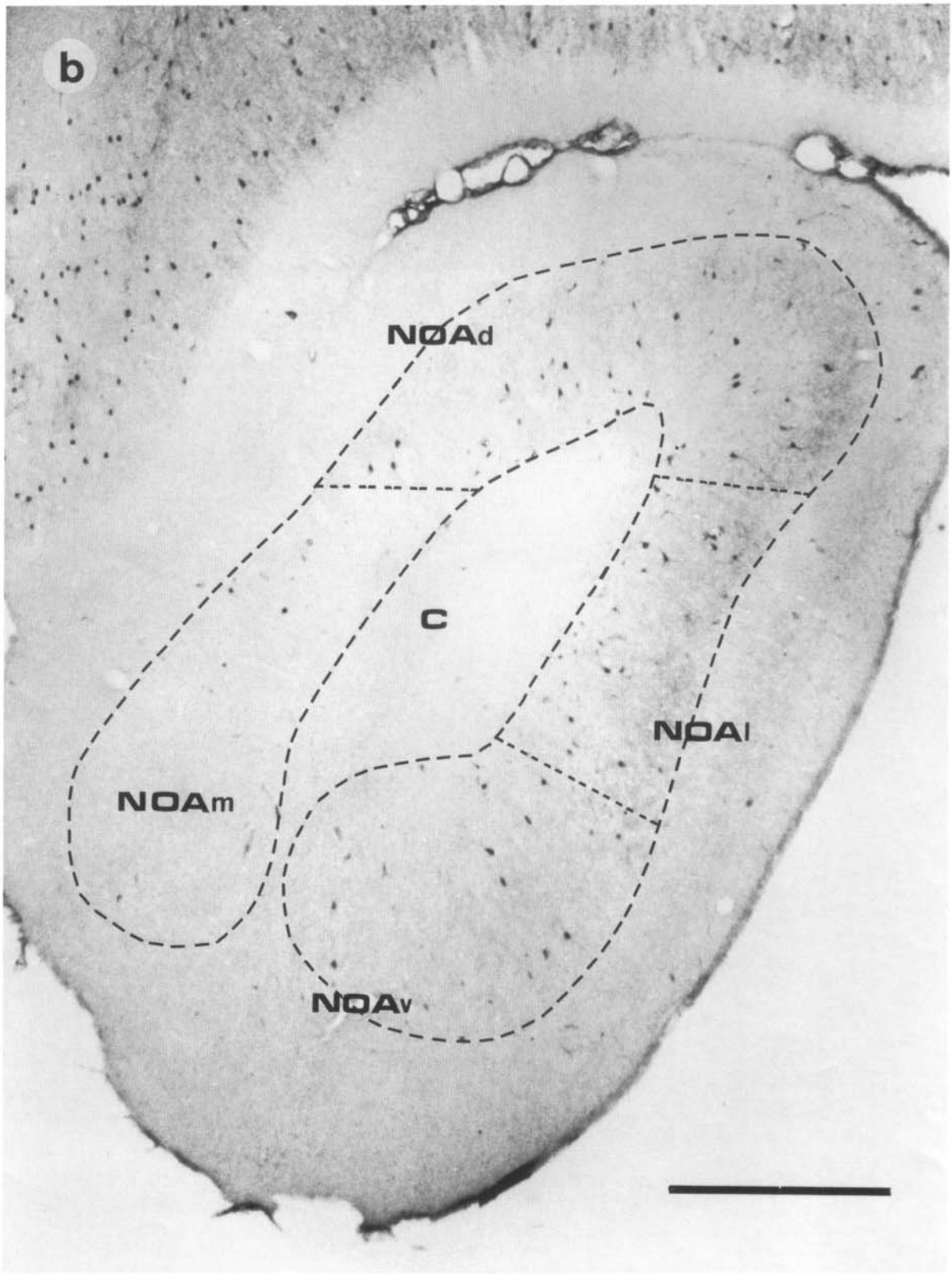
b
NOAd
C
NOAl
NOAm
NOAv

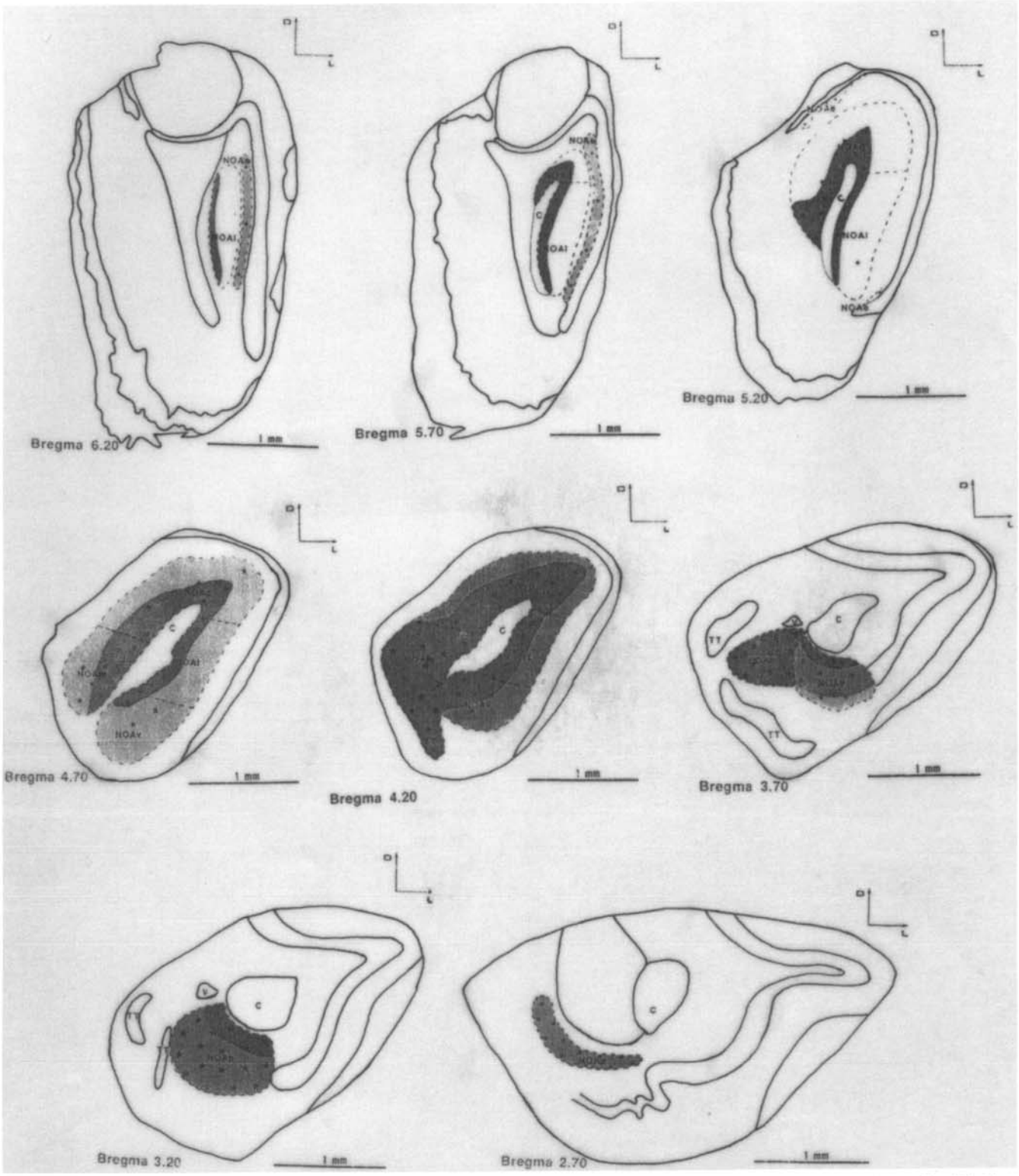

FIG. 2. Positive neuronal bodies are indicated by stars (large stars: high density: > 20 cell bodies; middle stars: intermediate density: 5–20 cell bodies; small stars: low density: < 5 cell bodies). Positive fibres are represented as follows: dark grid, high density; medium grid, intermediate density; light grid, low density. Camera lucida drawings of NOA frontal sections from the rostral (6.20) to caudal (2.70) Bregma levels, showing the location of CaBP-immunopositive elements. C: commissure. TT: taenia tecta. V: ventricle.

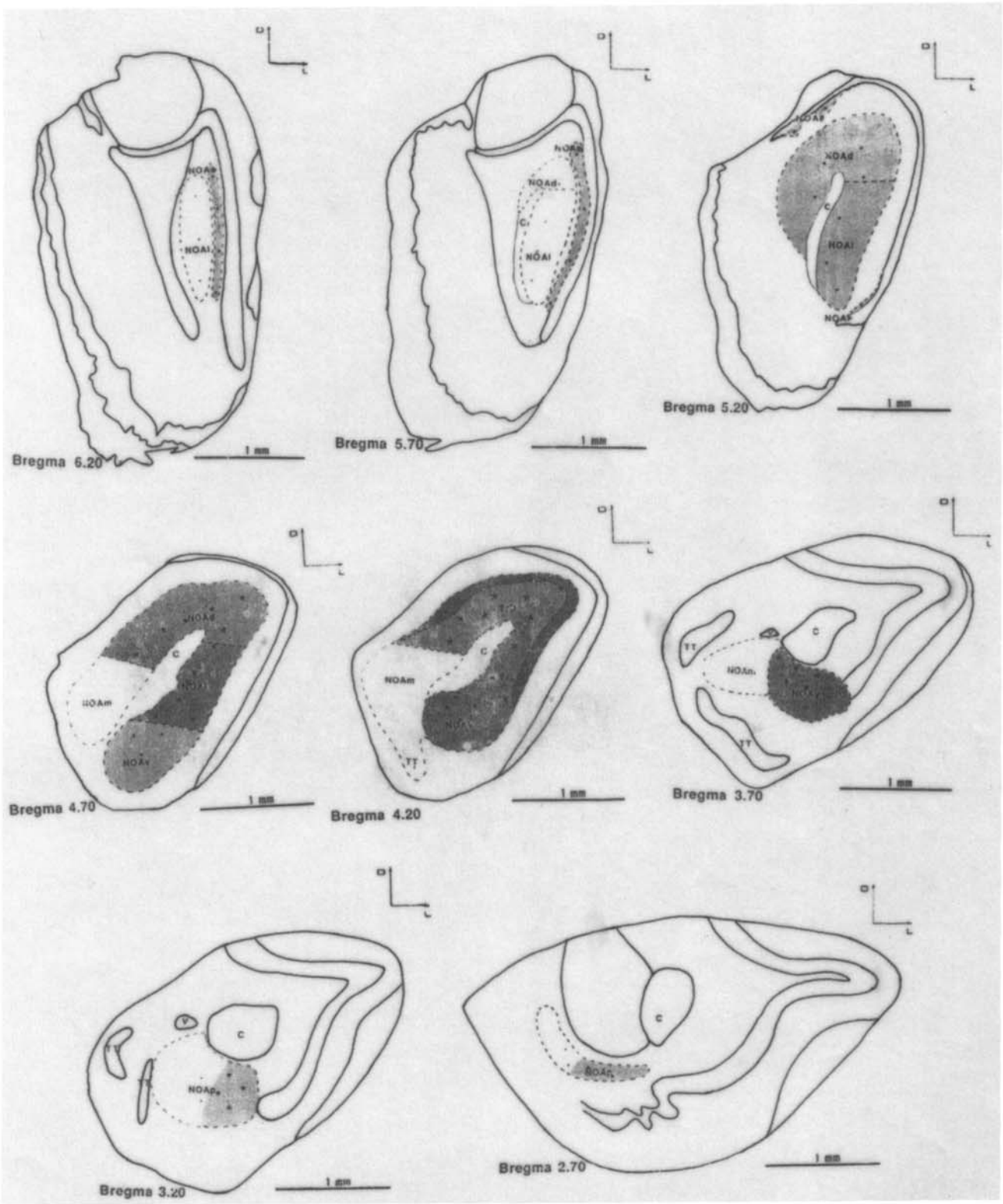

FIG. 3. Positive neuronal bodies are indicated by stars (large stars: high density: > 20 cell bodies; middle stars: intermediate density: 5-20 cell bodies; small stars: low density: < 5 cell bodies). Positive fibres are represented as follows: dark grid, high density; medium grid, intermediate density; light grid, low density. Camera lucida drawings of NOA frontal sections from the rostral (6.20) to caudal (2.70) Bregma levels, showing the location of PV-immunopositive elements. C: commissure. TT: taenia tecta. V: ventricle.

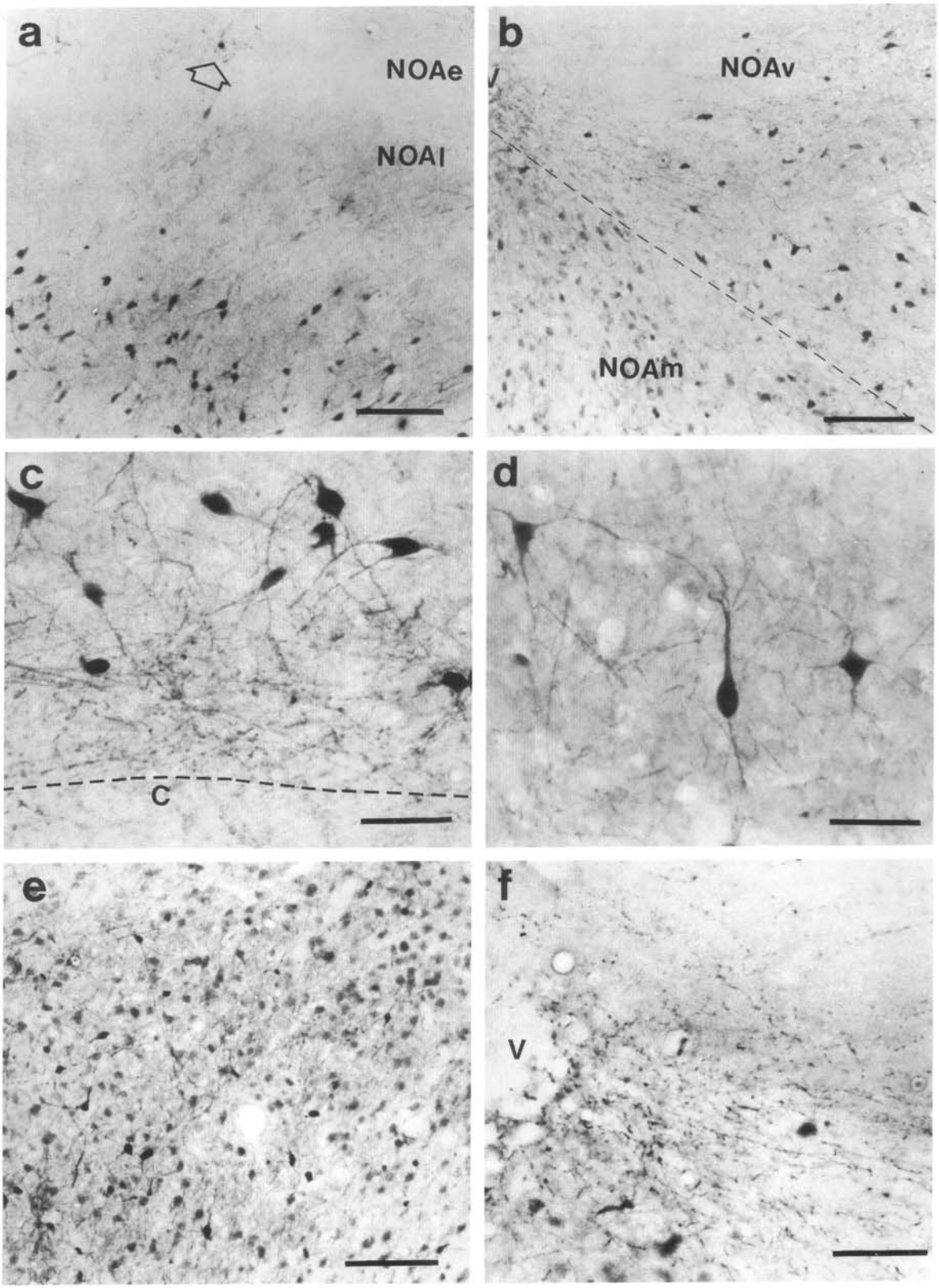

FIG. 4. CaBP-immunoreactivity. (a) Positive neurons and fibres in the NOAe and NOAl. Note the size differences between NOAe (arrow) and NOAl stained neurons. Scale bar = 100 μm. (b) Panoramic view of NOAv and NOAm. Note the lower density of positive elements in NOAv (V: ventricle). Scale bar = 100 μm. (c) Large density of varicose-positive fibers close to the commissure. Scale bar = 50 μm. (d) Heterogeneous morphologies in the NOAl (C: commissure). Scale bar = 50 μm. (e) Large density of immunostained fibres and irregular cell bodies in NOAp. Scale bar = 100 μm (f) Dense plexus of positive varicose fibres in NOAv, close to the ventricle (V: ventricle). Scale bar = 100 μm.

incubated by the avidin-biotin-peroxidase method (16). The sections were incubated with monoclonal antibody 235 against parvalbumin, and monoclonal antibody 300 against calbindin D-28K, diluted 1:2000 for 48 h followed, in both cases, by biotinylated antimouse immunogammaglobulin (Vectastain ABC kit, Vector Laboratories, Burlingame, USA) diluted 1:200 for 60 min at room temperature. Then, all sections were incubated with Vectastain ABC reagent diluted 1:225 for 90 min, also at room temperature. After two rinses in PB, peroxidase activity was revealed with 0.05% 3–3′ diaminobenzidine and 0.003% hydrogen peroxide in 0.2 *M* Tris buffer, pH 7.6.

Finally, the sections were mounted on slides, dehydrated in an increasing ethanol series, cleared with xylene, and coverslipped using Entellan.

Both used primary antibodies have been fully characterized (6,9). Additional controls of the immunostaining procedure were carried out as described previously (2).

The cell diameters were measured with a Zeiss ocular micrometer and the schemes of the different rat NOA levels were drawn using a camera lucida.

RESULTS

We have used the stereotaxic atlas of Paxinos and Watson (24) to fix the Bregma levels of our sections and the nomenclature used by De Olmos et al. (10) to describe the subdivisions and lamination of the rat NOA. Accordingly, we distinguished the following subdivisions: pars externa (NOAe), pars lateralis (NOAl), pars dorsalis (NOAd), pars ventralis (NOAv), pars medialis (NOAm), and pars posterioris (NOAp), as well as three transition areas: dorsalis (TrD), lateralis (TrL), and medialis (TrM).

No particular difference in the morphologies of CaBP- and PV-positive neurons and fibres was detected. However, there were significantly more CaBP-immunoreactive elements than PV-positive ones (Figs. 1, 2, 3).

Pars Externa

Calbindin D-28K and parvalbumin. Since the labellings for both calcium-binding proteins in this subdivision were very similar (Figs. 2, 3), we described them together. With both PV and CaBP antisera, we found a constant low staining in the NOAe. Positive cells (Fig. 4a) were scarce and sparse, they had small diameters (7–10 μm) and pyramidal shapes. An interesting feature of NOAe-stained cells was the absence of basal dendrites, whereas from the apical side arose two or three primary dendrites which were generally directed toward the lateral olfactory tract. In some PV-labelled cells we observed an axon-like prolongation coursing toward the inner zone of the olfactory peduncle (Fig. 5a).

In this subdivision we found scarce immunoreactive fibres for both PV and CaBP. They were short, little ramified, and sometimes varicose. These fibres formed small isolated plexuses and pericellular arrangements surrounding positive and negative cell bodies.

Pars lateralis

Calbindin D-28K. We observed in this subdivision an increasing gradient in the number and density of positive neurons and fibres following the rostrocaudal axis. First-labelled cell bodies occurred at Bregma level 5.70 and reached their highest density at Bregma 4.20. Most CaBP-stained somata were observed in the inner third of NOAl, close to the anterior commissure. More rarely, we observed isolated neurons located in the external region with their processes coursing parallelly at the NOAe–NOAl boundary.

The rostralmost CaBP-positive fibres in the NOAl were detected at Bregma level 6.20. These fibres were weakly labelled and occupied the inner part of this subdivision. At Bregma level 4.70 we observed a high density of immunoreactive fibres situated throughout the NOAl. In TrL, the staining showed a laminar appearance: an external band showing a medium density of positive fibres and a heavily immunostained band of CaBP fibres in the inner zone, coinciding with the labelled somata.

Parvalbumin. Only a few labelled neurons were visualized at Bregma levels 6.20, 5.70, and 5.20, an intermediate number at level 4.70 and, finally, at Bregma level 4.20, corresponding to the TrL, a larger immunoreactive neuronal population. Generally, all positive neurons were restrictly located in the zone close to the anterior commissure, with the exception of both first levels, where they were more widely distributed (Fig. 5c, 5d).

PV-positive fibres were also clearly observed. The rostralmost stained fibres in the NOAl appeared at Bregma level 5.20. They were scarce (Fig. 5c), but their density increased close to level 4.70. In more caudal sections, Bregma 4.20, which corresponded to the TrL, the immunoreactivity showed a laminar pattern: a strongly stained external band where few positive neurons can be seen, and an inner band with an intermediate density of labelled fibres where most PV neurons were located (Fig. 5d).

NOAl-stained neurons showed different shapes: fusiform, pyramidal, and polygonal (Fig. 4d), all of them with long dendritic processes which were sometimes ramified and varicose. The average size of NOAl cell bodies was larger than those of NOAe cells (Fig. 4a) and in the case of PV-positive fusiform cell bodies they reached 35 μm of major diameter.

The reactive fibres were long, rarely ramified, and those close to the anterior commissure, often varicose. These fibres showed no defined orientation. However, they were occasionally directed toward the commissure or distributed tangentially to this structure, forming a dense plexus surrounding it (Fig. 4c).

Pars Dorsalis

The distribution patterns of CaBP and PV in the NOAd were very similar to those previously described for the NOAl.

Calbindin D-28K. A moderate number of CaBP-stained neurons was distinguished at Bregma levels 5.20, 4.70, and 4.20. These somata occupied a larger extension than in NOAl and were located in the two inner thirds, although in the dorsolateral part of NOAd the immunopositive cells bodies appeared close to the external limit of this subdivision.

Concerning the CaBP-immunoreactive fibres, an abundant number was present at Bregma 5.70, coinciding their location with those of the positive somata previously described. On the contrary, in the rest of NOAd we have only observed a low density of stained fibres.

Parvalbumin The examination of PV-stained sections revealed scarce neuronal bodies at Bregma 5.70 and 5.20. An intermediate density was observed in more caudal levels. Normally, these somata were located in the same region that those CaBP positive. In the TrD, we found a much more abundant distribution of PV-reactive neurons. These cells occupied the two-thirds close to the anterior commissure, although just like in previous levels, they extended until the TrD external border in the dorsal zone.

At Bregma 5.20, some fibres appeared faintly stained. In TrD (Bregma 4.70) a moderate immunoreactivity was observed, with the exception of the lateral third, which was heavily labelled. The positive neuronal bodies were not located in this most re-

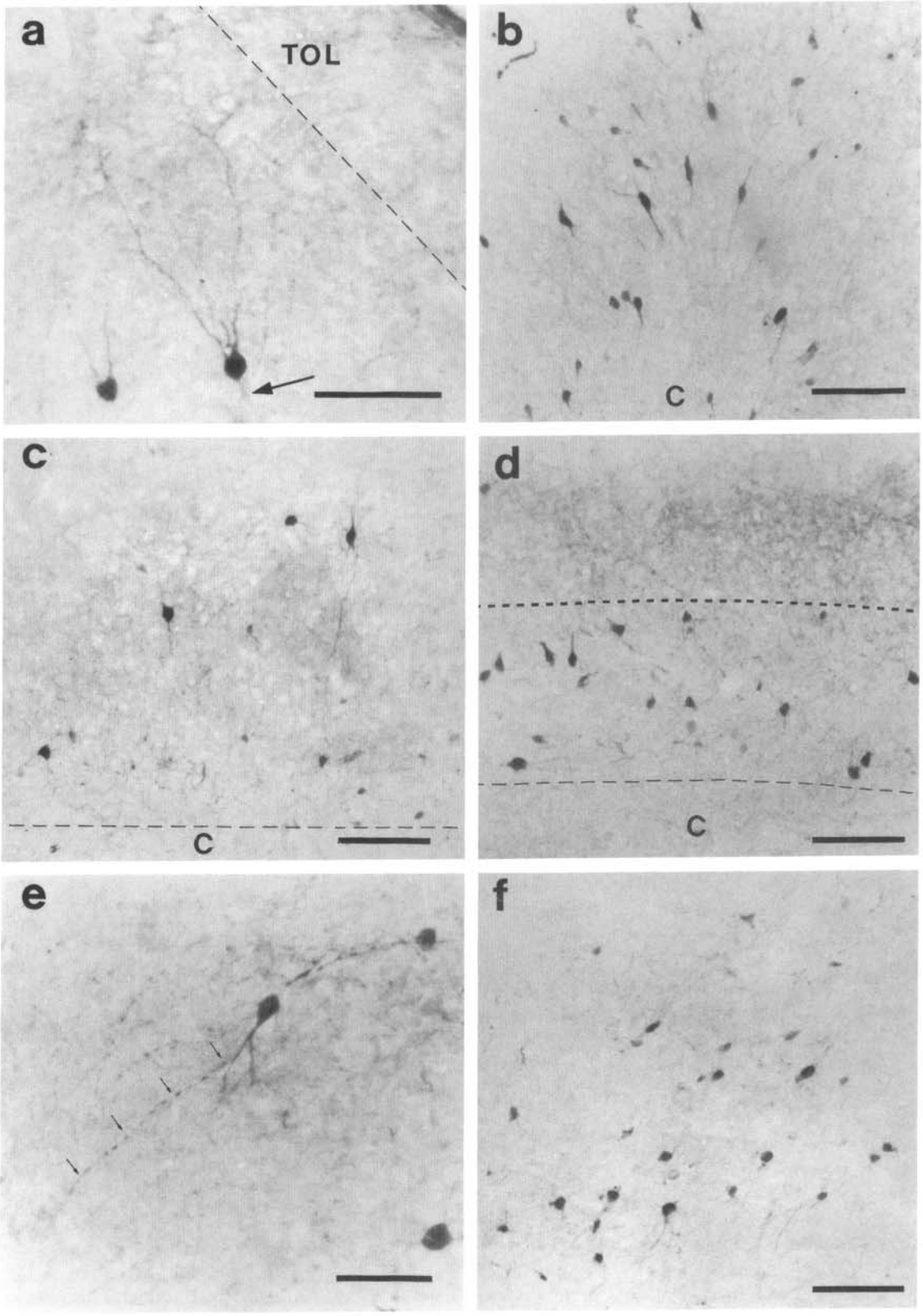
a
TOL
b
C
c
C
d
C
e
f

active lamina, except in the superior zone where we observed an intermediate quantity of PV fibres.

This subdivision contained mainly fusiform, pyramidal, and polygonal shaped neurons, with sizes similar to those of NOAl cells. Their long, rarely ramified, sometimes varicose dendrites were directed toward the anterior commissure (Fig. 5b).

The fibres were often varicose, especially close to the commissure, where they formed a dense fibrillar plexus. Occasionally, they were ramified, but we did not observe terminal fields.

Pars Ventralis

Calbindin D-28K. In the rostralmost region of NOAv (Bregma 4.70), some neurons were moderately stained for CaBP. They were located in the inner zone. More caudally, they increased their density and distribution and at Bregma level 3.70 the positive somata had a homogeneous distribution with a moderate density by all the extension of the subdivision (Fig. 4b).

A high density of CaBP-positive fibres was detected at Bregma level 4.70 close to the commissure, whereas only a low density in the rest. At Bregma 4.20 the half close to the commissure showed high immunoreactivity; however, in the band close to the lateral olfactory tract we have only seen a medium density. In the latter level, strongly stained fibres appeared in the inner zone, weakly stained in the external zone and moderately immunoreactive in the middle one.

Parvalbumin. At rostral levels, Bregma 4.70 and 4.20, scarce PV-stained neurons appeared in this subdivision. These cells occupied the dorsal inner region of NOAv. In Bregma 3.70, the caudalmost level of this subdivision, the distribution pattern of positive somata was similar, but they were more abundant.

Scattered PV-positive fibres were seen at 4.70 and with medium density in the following levels.

A large diversity of neuronal morphologies was seen in this pars: fusiform, piriform, pyramidal, and polygonal cells, generally radially oriented and with processes slightly divided, sometimes varicose (Fig. 5e) and directed toward the ventricle. Labelled fibres were also slightly ramified.

In the NOAv, contrary to other subdivisions, both slightly ramified fibres and dendrites were mostly oriented toward the ventricle where they formed a dense plexus of intermingled varicose processes (Fig. 4f).

Pars Medialis

Calbindin D-28K. We have seen a high CaBP-staining in this subdivision. It was notable the large number of positive somata and prolongations, endowing this subnucleus with a strong neuropil labelling. In the rostral part, a moderate number of neurons, located in the inner of NOAm, displayed CaBP immunoreactivity. At more caudal levels (Bregma 4.20 and 3.70) intense, abundant immunostained somata were found in practically all parts of the subnucleus (Fig. 4b), as well as an homogeneous, strongly stained neuropil. Neurons with fusiform and irregular morphologies were observed.

We found a high density of positive fibres in Bregma 4.20, Bregma 3.70, and in the inner half of Bregma 4.70, but only with medium density in the outer half of NOAm at this latter level.

In the rostral region, these fibres did not show a particular orientation, but more caudally we have seen a radial disposition. Frequently, the fibres presented varicosities, a main characteristic in the zone close to the anterior commissure and the ventricle. Around the ventricle these processes formed a dense plexus as in NOAv.

Parvalbumin We have not detected PV-immunopositive elements in the medial subnucleus, being NOAm the only PV-negative subdivision of the NOA (Fig. 1b).

The zone corresponding to the TrM showed similar labellings for both proteins to those observed in the adjacent NOAm (Figs. 2 and 3).

Pars Posterioris

The NOAp is the unique NOA subdivision at caudalmost Bregma levels (3.20 and 2.70).

Calbindin D-28K

We observed a strong CaBP immunoreactivity in NOAp at level 3.20, with a large number of labelled cell bodies (Fig. 4e), but more caudally (Bregma 2.70), positive neurons were moderate on the medial side and scarce on the lateral one.

The stained fibres appeared with medium density throughout the NOAp except close to the ventricle in Bregma 3.20, where there was a strong immunoreactivity.

Parvalbumin

The immunoreactivity pattern for this protein was very different between the medial and the lateral part. Only the lateral part showed a low density of labelled elements (somata and fibres) (Fig. 5f), whereas the medial side did not show positive staining (Fig. 3).

As described previously, the medial half of NOAp showed stainings for both proteins similar to those of NOAm (Figs. 2 and 3). Labelled somata presented generally irregular shapes (Fig. 4e) and, more rarely, fusiform morphologies oriented toward the ventricle. Positive fibres were short, varicose, and directed toward the ventricle where they formed a dense plexus.

DISCUSSION

In this study we described the distribution and morphology of PV- and CaBP-immunoreactive elements in the rat NOA. This brain center has been studied using different techniques such as Golgi impregnation (10,28,34), anterograde and retrograde tracers (1,14,15,20,21,27,30), and immunocytochemistry (8,12,13,32). Our study agrees well with the general structure and cytoarchitecture of the NOA reported in those previous studies. However, we have included in our study three transition areas: TrL, TrD, and TrM according to the followed nomenclature (10). De Olmos et al. (10) and Bayer (4) have defined these areas as laminated zones located between the NOA and the piriform cortex. Nevertheless, after CaBP and PV immunostainings only TrL and TrD, which were characterized by the beginning of a laminated structure and CaBP and PV labellings more similar to those of the olfactory cortex, were clearly observed. The

FIG. 5. PV immunoreactivity. (a) Two NOAe stained cells with their apical dendrites directed toward the tractus olfactorius lateral (TOL). (arrow: axon in the basal side). Scale bar = 50 μm. (b) Radially oriented stained neurons in NOAd. (C: commissure). Scale bar = 100 μm. (c) Unlaminated NOAl first levels. (C: commissure). Scale bar = 100 μm. (d) Two layers in TrL: an external with abundant positive fibres and an internal with most positive neurons. (C: commissure). Scale bar = 100 μm. (e) NOAv-positive cells with varicose dendrites (arrows). Scale bar = 50 μm. (f) PV immunostaining in NOAp. Note the difference with CaBP immunostaining. Scale bar = 100 μm.

TrM was indistinguishable in our preparations from the adjacent NOAm. Other authors (15,20,21,27,28) did not include transition areas in the rat NOA, but they considered a prepiriform cortex between the NOA and the piriform cortex. Paxinos (23) and Paxinos and Watson (24) described neither the transition areas nor a prepiriform cortex.

The medial half of NOAp showed CaBP and PV stainings more similar to those of NOAm than to the lateral half of NOAp. On the other hand, the distributions for PV and CaBP were comparable in all subdivisions with the exception of NOAm, which was CaBP positive and PV negative. Interestingly, the NOAm is the only NOA subdivision that projects almost exclusively ipsilaterally to the olfactory bulb (10,20,28).

Previous studies on the distribution of calcium-binding proteins in the whole rat brain (8,12,13,31,32) indicated the presence of PV and CaBP immunoreactivities in the NOA as appeared in our study. However, these general reports did not describe the morphologies of the positive elements as well as the distribution patterns in the different subdivisions. Thus, in addition to the presence of CaBP-labelled somata in all subdivisions of the NOA, we described different positive neuronal types, density variability into the different subdivisions, and a rostrocaudal increase in the density of stained neurons.

Feldman and Christakos (12), García-Segura et al. (13) and Séquier et al. (31,32) also distinguished the presence of CaBP-stained fibres, which has not been included in his study by Celio (8). These fibres were described with high density in the NOAm (12) in good agree with our results and with intermediate density in the rest of the NOA subdivisions. However, the distribution observed in our study is more complex, including low immunoreactive and immunonegative zones in these subdivisions.

It is necessary to be cautious in these comparisons with previous works on the distribution of the CaBP immunostaining because, except in the most recent publication (8), polyclonal antibodies against CaBP were used. These antisera present crossreaction with calretinin, another neuronal calcium-binding protein which possesses a primary sequence highly homologous to that of CaBP (29). The monoclonal CaBP antibody used in our study do not present crossreaction with calretinin (8).

With regard to PV, its presence in the rat NOA has been only reported by Celio (8), who observed large stained cells in the rostral part of NOAv, NOAl and NOAd, but not in NOAm, according with our results. At more caudal levels, however, he described parvalbuminergic cells in the NOAm, which have not been detected in our study. Another difference concerns with the presence of PV-positive fibres, widely distributed in the rat NOA and not reported by this author.

The CaBP- and PV-stained neurons in NOAe were different from the positive cells in the other NOA subdivisions. These smaller neurons, with oriented dendritic trees have also been described using silver impregnation (15,28,34). In the rest of rat NOA subdivisions most authors found pyramidal cells as the main neuronal type (15,34). However, other neurons with fusiform and polygonal shapes, also observed by us, have been described using Golgi impregnation (28). It suggests that both CaBP- and PV-positive populations in the NOA are complex groups including different neuronal types.

In relation with the distribution in the rat NOA of the above-cited calcium-binding protein calretinin, some differences between its localization and that from CaBP were evident. Whereas we found a low density of CaBP-positive elements throughout the NOAe, the distribution of calretinin is more heterogeneous with a large number of positive cells only located at its ventralmost zone. Furthermore, contrary to our observations with the anti-CaBP antiserum, the NOAl was mostly devoid of calretinin-stained fibers. Thus, we can conclude that all three proteins: CaBP, PV, and calretinin, which are specific for neuronal subpopulations, were present in the rat NOA but with different distribution patterns.

Finally, CaBP- and PV-like immunoreactivities have been noticed in the human NOA (22). Staining intensity and number of CaBP-positive neurons increased in the peripheral-central and rostro-caudal axis, as we have observed in the rat. Interestingly, Ohm et al. (22) described for both proteins entirely complementary distributions in both intrabulbar and intrapeduncular portions of the NOA. In the rat, on the contrary, we found an extense overlapping between the distribution of both proteins. However, whether the same neurons in each subdivision colocalize both proteins or are different populations with a quite similar distribution remains unknown and should be object of future studies.

ACKNOWLEDGEMENTS

The authors want to express their gratitude to Prof. Dr. M. R. Celio for kindly providing the specific antibodies. This work was supported by the University of Salamanca (grants to J. R. Alonso and J. Aijón) and by a DGICyT project (PB91/0424).

REFERENCES

1. Alheid, G. F.; Carsel, J.; de Olmos, J.; Heimer, L. Quantitative determination of collateral olfactory nucleus projection using a fluorescent tracer with an algebraic solution to the problem of double labelling. Brain Res. 292:17–22; 1984.
2. Alonso, J. R.; Arévalo, R.; Briñón, J. G.; Lara, J.; Weruaga, E.; Aijón, J. Parvalbumin immunoreactive neurons and fibres in the teleost cerebellum. Anat. Embryol. 185:355–361; 1992.
3. Baimbridge, K. G.; Miller, J. J.; Parkes, C. O. Calcium-binding protein distribution in the rat brain. Brain Res. 239:519–525; 1982.
4. Bayer, S. A. Neurogenesis in the anterior olfactory nucleus and its associated transition areas in the rat brain. Neuroscience 4:225–249; 1985.
5. Brederode, J. F. M. van; Mulligan, K. A.; Hendrickson, A. E. Calcium binding proteins as markers for subpopulations of GABA-ergic neurons in monkey striate cortex. J. Comp. Neurol. 298:1–22; 1990.
6. Celio, M. R.; Baier, W.; Schärer, L.; de Viragh, P. A.; Gerday, C. Monoclonal antibodies directed against calcium binding protein parvalbumin. Cell Calcium 9:81–86; 1988.
7. Celio, M. R. Calcium binding protein in the brain. Arch. Ital. Anat. Embriol. 94:227–239; 1989.
8. Celio, M. R. Calbindin D-28K and parvalbumin in the rat nervous system. Neuroscience. 35:375–475; 1990.
9. Celio, M. R.; Baier, W.; Schärer, L.; Gregersen, H. J.; de Viragh, P. A.; Norman, W. A. Monoclonal antibodies directed against the calcium binding protein calbindin D-28K. Cell Calcium 11:599–602; 1990.
10. De Olmos, J.; Hardy, H.; Heimer, L. The afferent connections of the main and accessory olfactory formations in the rat: An experimental HRP-study. J. Comp. Neurol. 181:213–244; 1978.
11. Endo, T.; Takazawa, K.; Kobayashi, S.; Onaya, T. Immunochemical and immunohistochemical localization of parvalbumin in rat tissues. J. Neurochem. 46:892–898; 1986.
12. Feldman, S. C.; Christakos, S. Vitamin D-dependent calcium-binding protein in the rat brain: Biochemical and immunocytochemical characterization. Endocrinology 112:290–302; 1982.
13. García-Segura, L. M.; Baetens, D.; Roth, J.; Norman, A. W.; Orci, L. Immunohistochemical mapping of calcium-binding protein immunoreactivity in the Central Nervous System. Brain Res. 296:55–63; 1984.

14. Haberly, L. B.; Price, J. L. The axonal projection patterns of the mitral and tufted cells of the olfactory bulb in the rat. Brain Res. 129:152–157; 1977.
15. Haberly, L. B.; Price, J. L. Association and commissural fiber system of the olfactory cortex of the rat. II. Systems originating of the olfactory peduncle. J. Comp. Neurol. 181:781–808; 1978.
16. Hsu, S.-M.; Raine, L.; Fanger, H. Use of avidin-biotin-peroxidase complex (ABC) in immunoperoxidase techniques: A comparison between ABC and unlabeled antibody procedures. J. Histochem. Cytochem. 29:577–580; 1981.
17. Jacobowitz, D. M.; Winsky, L. Immunocytochemical localization of calretinin in the forebrain of the rat. J. Comp. Neurol. 304:198–218; 1991.
18. Jande, S. S.; Maler, L.; Lawson, D. E. M. Immunohistochemical mapping of vitamin D-dependent calcium-binding protein in rat brain. Nature 294:765–767; 1971.
19. Khanna, N. C.; Tokuda, M.; Waisman, D. M. The role of calcium binding proteins in signal traduction. In: Cooke, B. A.; King, R. J. B.; van der Molen, H. J., eds. Hormones and their actions. Part II. Amsterdam: Elsevier; 1988:63–92.
20. Luskin, M. B.; Price, J. L. The topographic organization of associational fibers of the olfactory system of the rat, including centrifugal fibres to the olfactory bulb. J. Comp. Neurol. 216:264–291; 1983.
21. Luskin, M. B.; Price, J. L. The laminar distribution of the intracortical fibers originating in the olfactory cortex of the rat. J. Comp. Neurol. 216:292–302; 1983.
22. Ohm, T. G.; Müller, H.; Braak, E. Calbindin-D-28K-like immunoreactive structures in the olfactory bulb and anterior olfactory nucleus of the human adult: Distribution and cell typology Partial complementarity with parvalbumin. Neuroscience 42:823–840; 1991.
23. Paxinos, G. The rat nervous system. Vol 1. Forebrain and midbrain. Sydney: Academic Press; 1985:14–19.
24. Paxinos, G.; Watson, C. The rat brain in stereotaxic coordinates. Sydney: Academic Press; 1986.
25. Persechini, A.; Moncrief, N. D.; Kretsinger, H. The EF-hand family of calcium-modulated proteins. Trends Neurosci. 12:462–467; 1989.
26. Pinol, M. R.; Kägi, U.; Heizmann, C. W.; Vogel, B.; Séquier, J. M.; Haas, W.; Hunzinker, W. Poly- and monoclonal antibodies against recombinant rat brain calbindin D-28K were produced to map its selective distribution in the Central Nervous System. J. Neurochem. 54:1827–1833; 1990.
27. Price, J. L. An autoradiographic study of complementary laminar patterns of termination of afferent fibers to the olfactory cortex. J. Comp. Neurol. 150:87–108; 1973.
28. Reyher, C. K.; Schwerdtfeger, W. K.; Baumgarten, H. G. Intrabulbar axonal collateralization and morphology of anterior olfactory nucleus neurons in the rat. Brain Res. Bull. 20:549–566; 1988.
29. Rogers, J. M. Calretinin: A gene for a novel calcium-binding protein expressed principally in neurons. J. Cell Biol. 105:1343–1353; 1987.
30. Schowb, J. E.; Price, J. L. The development of axonal connections in the central olfactory system of the rats. J. Comp. Neurol. 223: 177–202; 1984.
31. Séquier, J. M.; Hunzinker, W.; Richards, G. Localization of calbindin D28 mRNA in rat tissues by in situ hybridization. Neurosci. Lett. 86:155–160; 1988.
32. Séquier, J. M.; Hunzinker, W.; Andressen, C.; Celio, M. R. Calbindin D-28K protein and mRNA localization in the rat brain. Eur. J. Neurosci. 2:1118–1126; 1990.
33. Somogyi, P.; Takagi, H. A note on the use of picric acid-paraformaldehyde-glutaraldehyde fixative for correlated light and electron microscopic immunocytochemistry. Neuroscience 7:1779–1784; 1982.
34. Valverde, F. The nucleus olfactorius anterior and the commissura anterior. In: Studies on the piriform lobe. Cambridge, MA: Harvard University Press; 1965:54–61.